Electric Noise Spectra of a Near-Surface Nitrogen-Vacancy Center in Diamond with a Protective Layer

Philip Chrostoski,[1,*] H. R. Sadeghpour,[2] and D. H. Santamore[1,2]

[1] *Department of Physics and Engineering Physics, Delaware State University, Dover, Delaware 19901, USA*
[2] *ITAMP, Harvard-Smithsonian Center for Astrophysics, Cambridge, Massachusetts 02138, USA*

(Received 16 April 2018; revised manuscript received 23 August 2018; published 21 December 2018)

Surface noise is a detrimental issue for sensing devices based on shallow nitrogen-vacancy (N-V) color-center diamonds. A recent experiment indicates that electric-field noise is significant compared to magnetic-field noise. They also found that the electric-field noise can be reduced with a protective surface layer, although the mechanism of noise reduction is not well understood. We examine the effect of a protective surface layer on the noise spectrum, which is caused by surface-charge fluctuations. We use the fluctuation-dissipation theorem to calculate and analyze the noise spectrum for six different surface-layer materials typically used for N-V-center diamond devices. We find that four parameters largely affect the noise spectrum: the effective relaxation time, the effective loss tangent, the power-law exponent of the noise spectrum, and the layer thickness. Our results suggest that a surface-covering layer is indeed useful for decreasing surface noise, but which material is most suitable depends on the device operational frequency range.

DOI: 10.1103/PhysRevApplied.10.064056

I. INTRODUCTION

Nitrogen-vacancy- (N-V)-center diamonds are attractive candidates for a wide range of applications, ranging from quantum metrology and sensing to quantum information processing and hybrid quantum systems [1,2]. Much of the interest in N-V-center diamonds stems from the long quantum-coherence time of their spin states—several milliseconds at temperatures well above room temperature [3]—and their extremely high sensitivity to electric and magnetic fields [4–9]. N-V color centers have a number of practical applications [10–27] in magnetic-field sensing, magnetometry, scanning thermal microscopy, and frequency-modulated radio reception in extreme conditions, in addition to being candidates for room-temperature quantum computing.

When functioning as detectors, N-V centers must be placed as close to the sample surface as possible, for maximal detection sensitivity [28–33]. Yet room-temperature devices with N-V centers near the surface tend to be noisy. This noise produces fluorescent line-broadening and decreases the overall detection sensitivity. Previously, magnetic-field noise has been regarded as a dominating source of noise [34–37]. The majority of magnetic-field noise comes from bulk-impurity interactions of nuclear and electronic spin baths [38,39]. Surface magnetic noise also exists and has been attributed to electron spins of dangling bonds [40,41], terminating surface atoms [42,43], absorption of molecules [44], and interactions with paramagnetic surface molecules [45]. Magnetic surface states have been experimentally observed for both bulk- and single-crystalline surfaces [36,46,47].

However, recent experiments by Kim *et al.* [32] and Romach *et al.* [48] have revealed that, in devices at room temperature, electric-field fluctuations can sometimes be a larger source of noise than magnetic-field fluctuations. The electric-field noise may be caused by lattice strain [9] and dipole fluctuations of an N-V center due to interaction with fluctuating surface charges, although the effect of the former seems to be much smaller than that of the latter. Mamin *et al.* [49] were able to reduce N-V-center noise by placing a layer of polymethyl methacrylate atop the diamond. Kim *et al.* [32] also reported noise-spectrum and T_2 coherence-time improvement with certain covering materials on N-V-center diamonds. Other materials, however, either reduce or increase surface noise [48,50–52]. Until now, there has been no systematic theoretical study of electric noise in N-V-center-diamond devices with different covering layers, nor any heuristics beyond experimental intuition for determining which materials efficiently reduce noise in which frequency bands.

In this paper, we study the physics of surface electric-field noise in diamonds containing N-V centers. We evaluate the effect of noise reduction with a liquid or solid cover layer and identify the parameters that control noise reduction in various situations. Since most N-V-center

*pcchrostoski16@students.desu.edu

devices operate at room temperature, we treat the surface electric-field noise as being produced mainly by thermally activated fluctuating dipoles caused by the surface charges. These dipole fluctuations lead to fluctuations in the electric field at the position of the color center. We use the fluctuation-dissipation theorem for noise calculations. Kuehn *et al.*, for example, have used the method to calculate the dielectric fluctuation due to noncontact friction for polymethyl methacrylate (PMMA) [53] at a fixed frequency. We use it to calculate frequency-dependent noise with different covering materials to explore the optimal frequencies of operation for those materials.

Our theoretical model, described in Sec. II, consists of a diamond coated with a cover layer, which we also sometimes refer to as a "protective layer." We use the fluctuation-dissipation theorem to obtain noise spectra at room temperature, and we calculate the effective capacitance and loss tangent. The surface cover materials that we consider are glycerol, propylene carbonate (PC), polymethyl methacrylate (PMMA), polyvinylindene fluoride (PVDF), perfluoropolyether (PFPE), and dimethyl sulfoxide (DMSO). PMMA, PVDF, PFPE, glycerol, and PC have been commonly used in experimental work [48–52]. PMMA and PVDF are both solids, while all the others are liquid at room temperature. We analyze the noise spectra at frequencies ranging from 1 kHz to 10 MHz, typical in experiments, and compare the results with the experimental data of Ref. [32].

We find that there are four main parameters that shape the noise spectrum: the effective relaxation time, the effective loss tangent, the coefficient of the power law of the noise spectrum, and the thickness of the surface layer. The effective capacitance also matters, but to a lesser extent. In Sec. III, we examine the role of each parameter in depth and discuss how the protective layer affects the parameters and the shape of the noise spectrum. The effective relaxation time τ_{eff} determines the transition frequency of the noise spectrum.

Our study of six experimentally representative covering materials shows that most covering materials commonly used by experimentalists can reduce noise in the frequency range of interest. Most liquid surface layers are much better than solid layers at reducing noise. This is because liquid layers have shorter (picosecond to nanosecond) characteristic relaxation times than solid layers (microseconds). However, the power-law exponent for liquids is in general smaller than that for solids and is greatly affected by the thickness.

The frequency range in which the power law dominates the noise spectrum is narrower for liquids than for solids. In liquids, a constant noise floor (i.e., white noise) reappears at frequencies above 10^5–10^6 Hz, while the noise spectrum in solids still follows the power law in this frequency range. As a result, at around 1 MHz, solids start to perform better in noise reduction than some liquids. At high frequencies ($>10^7$ Hz), a solid protective layer will outperform all liquid layers in noise reduction. The thickness of the surface layer affects the amount of noise: in general, thinner protective layers reduce the white-noise floor better than thick protective layers.

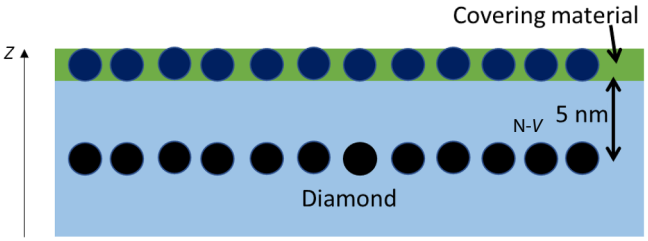

FIG. 1. The model consists of diamond with an N-V center placed 5 nm below the surface and a protective layer covering the surface of the diamond. The lower black dots represent the N-V center, while the upper blue dots represent the free positive charge of the protective material.

II. THE MODEL AND CALCULATIONS

A. The noise spectrum

Our model consists of a room-temperature diamond with an N-V center embedded 5 nm below the diamond surface, with a liquid or solid layer covering the surface (see Fig. 1).

The covering materials that we investigate are glycerol, PC, PMMA, PVDF, PFPE, and DMSO. The reason for choosing these different materials is their favorable characteristics. For example, Kim *et al.* [32] have shown that glycerol does not affect the dark spin density of N-V centers even though glycerol's hydroxyl groups can donate protons and possibly passivate dangling electrons. On the other hand, propylene carbonate and DMSO are aprotic solvents with tightly bound atoms and are optically transparent in the wavelength regimes of N-V-center experiments. PMMA, PVDF, and PFPE are all nonreactive, thermally stable, and optically transparent [54–57]. PFPE has been used in space-based applications for its optical transparency, and PMMA acts like normal window glass, only filtering out wavelengths below 300 nm.

We assume that the N-V centers are far apart and do not interact with each other. We focus on the noise above the N-V centers and ignore the noise below them, since we are interested in noise reduction at the surface due to various protective layers. The noise from below the N-V centers is the same for all covering layers, and so this noise source is not relevant for comparative noise reduction.

The interaction Hamiltonian of this system is

$$H_{\text{int}} = -\mathbf{p} \cdot \mathbf{E}, \tag{1}$$

where $\mathbf{p}$ is the electric dipole moment between the free positive charges in the covering liquid and the N-V-center electron and $\mathbf{E}$ is the electric field.

We want to find the noise spectrum, $S(\mathbf{k},\omega)$, arising from the fluctuation of the dipole moment between the N-V center and the covering layer. The electric field is due to charge fluctuations and acts on the system through the dipole moment. To obtain the noise spectrum, it is necessary to calculate the two-point space-time correlation of the dipole moment fluctuation, $\langle \delta p(\mathbf{r},\tau)\delta p(\mathbf{r}',\tau+t)\rangle$, and then calculate the noise spectrum by means of

$$S(\mathbf{k},\omega) = 2\int_{-\infty}^{\infty} \langle \delta p(\mathbf{r},\tau)\delta p(\mathbf{r}',\tau+t)\rangle e^{-i\omega t}dt. \quad (2)$$

However, since the system's response function is local, fluctuations at distinct spatial coordinates are uncorrelated. Then $\delta p(\mathbf{r},\tau) = \delta p(\tau)$ and $S(\mathbf{k},\omega) = S(\omega)$. Using the fluctuation-dissipation theorem (for details, see the Appendix), we obtain

$$S(\omega) = \frac{4\hbar}{1-e^{-\hbar\omega/k_BT}}\varepsilon_0\chi_e'',$$

where χ_e'' is the imaginary part of the complex electric susceptibility, k_B is the Boltzmann constant, and T is the temperature.

Let ε' and ε'' be the real and imaginary parts of the permittivity. We rewrite $\varepsilon_0\chi_e''$ in terms of the loss tangent, $\tan\phi(\omega) \equiv \varepsilon'/\varepsilon''$, from the complex permittivity

$$\varepsilon_0\chi_e''(\omega) = \varepsilon'(\omega)\tan\phi(\omega). \quad (3)$$

We choose the axis of interaction of $\mathbf{p}$ to be the z axis, as shown in Fig. 1, and model the two layers above the N-V center—the diamond and cover layers—each with capacitance C. The system is analogous to parallel-plate capacitors in series due to the intrinsic electric field naturally generated by the dipole interactions between the negative charge in the N-V center and the positive charge in the covering layer. After some manipulation, the noise spectrum per unit volume becomes

$$\bar{S}(\omega) = \frac{4\hbar C(\omega)}{1-e^{-\hbar\omega/k_BT}}\tan\phi(\omega). \quad (4)$$

B. The effective capacitance and effective loss tangent

Equation (4) contains the capacitance $C(\omega)$ and loss tangent, $\tan\phi(\omega)$. The capacitance is expressed in terms of the electric field as $C(\omega) = 1/E(\omega)d$, with

$$E(\omega) = \frac{\kappa q}{\varepsilon'(\omega)\,d^2}, \quad (5)$$

where $\kappa = 1/4\pi\varepsilon_0$, q is the charge, and d is the thickness of the layer. This expression allows us to write the capacitance in terms of electric permittivity. The frequency-dependent permittivity for a single material is a relaxation permittivity, given by the Havriliak-Negami relaxation function [58]

$$\varepsilon(\omega) = \varepsilon_\infty + \frac{\triangle\varepsilon}{[1+(i\omega\tau)^\gamma]^\beta}, \quad (6)$$

where $\triangle\varepsilon = \varepsilon_\infty - \varepsilon_s$ is the difference between the limiting high-frequency permittivity ε_∞ and the limiting low-frequency "static" permittivity ε_s, and τ is the medium's characteristic relaxation time, given in terms of the material's relaxation frequency f_r by $\tau = 1/2\pi f_r$. The exponents γ and β are fractional shape parameters describing the skewing and broadening of the dielectric function.

For a diamond without any protective layer, the capacitance $C(\omega)$ and loss tangent $\tan\phi(\omega)$ in Eq. (4) are simply calculated from the properties of diamond. However, with a protective layer on the surface, we need to compute and use an effective capacitance $C_{\text{eff}}(\omega)$ and loss tangent $\tan\phi_{\text{eff}}(\omega)$ to calculate $\bar{S}(\omega)$. We model the structure as a "covering layer" above the top diamond layer (i.e., the 5 nm diamond layer directly above the N-V center). Then, the effective loss tangent $\tan\phi_{\text{eff}}(\omega)$ is given by [59–62]

$$\tan\phi_{\text{eff}}(\omega) = b_H d_H \tan\phi_H(\omega) + b_L d_L \tan\phi_L(\omega), \quad (7)$$

where H and L, respectively, denote the higher and lower index of refraction of the surface liquid and the top diamond layer. The coefficients d_L and d_H are the thicknesses of the two materials, and

$$b_{L,H} = \frac{1}{\sqrt{\pi}w}\left(\frac{Y_{L,H}}{Y_s} + \frac{Y_s}{Y_{L,H}}\right), \quad (8)$$

where w is the width and $Y_{L,H,s}$ is the Young's modulus. The subscript s refers to the substrate, that is, the diamond below the N-V center. We have written this formula as $Y_{L,H,s}$ even though $s = L$ or $s = H$—either the L layer or the H layer is diamond, as is the substrate—so that Eq. (8) can be used for two different covering layers on the diamond surface if needed. The effective capacitance $C_{\text{eff}}(\omega)$ is the capacitance of the two layers of dielectric materials, equivalent to the diamond and the protective layer in series. The material parameters used in our calculations are taken from the literature [63–70] and are shown in Table I.

TABLE I. The material parameters used in Eqs. (8) and (6).

Material	ε_s	ε_∞	Y (GPa)	τ (ns)	γ	β
Diamond	7.99	5.7	443	2480	0.97	0.89
Glycerin	51.8	3.9	4.80	19.9	1.00	0.67
PC	64.9	4.7	8.09	0.0433	0.985	0.927
DMSO	45.9	6.36	4.50	11.0	1.00	1.00
PMMA	3.60	2.6	5.00	500	1.00	1.00
PVDF	7.50	5.0	1.10	100 000	1.00	1.00
PFPE	104	5.0	34.5	7.00	0.87	1.00

III. RESULTS AND DISCUSSION

Figure 2 shows the calculated noise spectra as a function of frequency for bare diamonds and for diamonds with various surface-protective layers of thickness 5 nm.

At low frequencies the noise spectra exhibit white noise, with a transition at higher frequencies to a power-law spectrum, with $S(\omega) \propto 1/f^{a}$. This agrees with the experimental findings of Romach *et al.* [48]. White noise at low frequencies comes about when dipoles try to align themselves into an equilibrium state.

We see from Fig. 2 that all of the surface-covering materials that we examine reduce the noise in some though not all frequency ranges. This agrees with the experimental observations reported for glycerin and propylene carbonate by Kim *et al.* [32]. However, certain materials are more effective in reducing noise at low frequencies, while others work better at high frequencies. For example, PVDF generates more noise than bare diamond at frequencies less than 3×10^4 Hz but surpasses PMMA in noise reduction above 2×10^5 Hz, glycerol above 4×10^5 Hz, and PFPE above 10^6 Hz.

Four parameters largely affect the shape of the noise spectrum at room temperature: the effective relaxation time τ_{eff}, the effective loss tangent $\tan\phi_{\text{eff}}(\omega)$, the power-law coefficient a, and the thickness of the surface layer. The effective capacitance also affects the noise spectrum; however, the effect is minimal compared to the other parameters, because of very little variation of the real permittivity ϵ' with frequency (see Sec. III B).

A. The effective relaxation time

The effective relaxation time τ_{eff} determines the transition frequency f_t at which the spectrum transitions from white noise to a power law. The relationship is $f_t = 2\pi/\tau_{\text{eff}}$, where $1/\tau_{\text{eff}} = 1/\tau_{\text{dia}} + 1/\tau_{\text{surf}}$. Here, τ_{dia} and τ_{surf} are the material relaxation times of the diamond and the protective surface layer, respectively. Thus, for a liquid-surface protective layer, in which $\tau_{\text{surf}} \gg \tau_{\text{dia}}$, the effective transition time is predominantly determined by the relaxation time of the diamond. With a solid surface, on the other hand, τ_{surf} is comparable to τ_{dia}, and thus the effective relaxation time will be determined by both τ_{surf} and τ_{dia}. We discuss the effect of thickness in Sec. III D.

B. The effective loss tangent

Figures 2 and 3(a) show that the amount of white noise is determined by the effective loss tangent $\tan\phi_{\text{eff}}(\omega)$. In addition, the overall charge-fluctuation noise is proportional to the dielectric loss tangent, and thus the charge-fluctuation noise increases for lossy materials.

Next, since the loss tangent is defined as the ratio of the imaginary permittivity ϵ'' to the real permittivity ϵ', we look into both ϵ' and ϵ''. Compared to the imaginary part [see Fig. 3(a)], the real part of the permittivity is relatively constant with frequency throughout the frequency range 10^3–10^7 Hz, except around the transition frequency f_t [see Fig. 3(b)]. As a result, $\tan\phi_{\text{eff}}(\omega)$ is predominantly determined by the imaginary permittivity. This could be why Kim *et al.* [32], who used only real permittivity to estimate the noise, could not explain the noise spectra that they observed in their experiments.

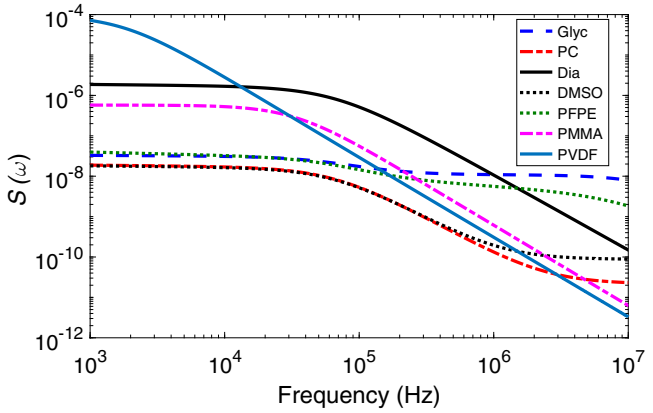

FIG. 2. The charge noise spectrum: bare diamond (black); with glycerol (blue dashed); with propylene carbonate (red dashed); with dimethyl sulfoxide (black dotted); with perfluoropolyether (green dotted); with polyvinylidene fluoride (navy); and with polymethyl methacrylate (pink dashed). The N-V-center diamond with a liquid protective layer exhibits better noise reduction than the bare diamond and the diamond with a solid protective layer in the frequency range $<10^6$ Hz.

The noise spectrum is also affected by the capacitance, as shown in Eq. (4), and thus it is also proportional to the real part of the permittivity. However, since the real permittivity is relatively constant with frequency, except around the transition frequency f_t, the effect of capacitance on the noise spectrum is much less than that of the loss tangent.

C. The power-law exponent

In atomic systems such as an ion trap, the power law $1/f^{a}$ is associated with the number of excitation modes of environmental phonons [71]. However, in our study, temperature is held constant and thus the excitation modes of environmental phonons are the same for all materials. As can be read off from Fig. 2, the noise spectra of the solid systems that we consider (bare diamond, PVDF + diamond, and PMMA + diamond) follow a power law with an exponent ranging from $a = -2.1$ to $a = -2$. On the other hand, with a liquid surface layer such as glycerin, PC, DMSO, and PFPE, the power-law exponent varies from $a = -0.5$ to $a = -1.9$. The exponent depends on the thickness, as discussed in Sec. III D.

D. The thickness of the surface layer

Table II shows that for liquid surface layers, the power-law exponent a varies drastically with thickness. For

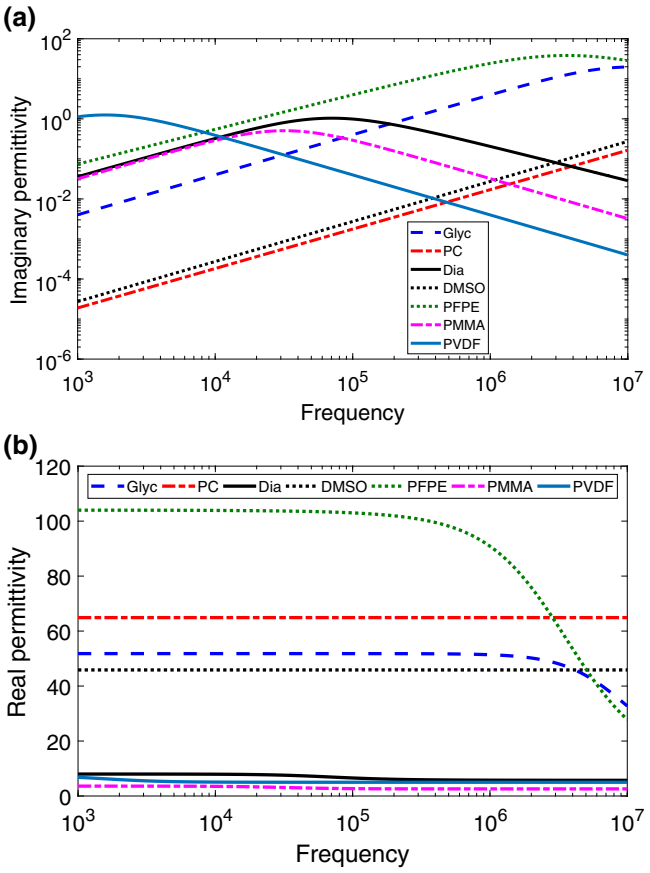

FIG. 3. The (a) imaginary and (b) real permittivities as a function of frequency: bare N-V-center diamond (black); with glycerol (blue dashed); with propylene carbonate (red dashed); with dimethyl sulfoxide (black dotted); with perfluoropolyether (green dotted); with polyvinylidene fluoride (navy); and with polymethyl methacrylate (pink dashed). The real part of the permittivity is almost constant with frequency, except at frequencies around $1/\tau$.

solid surface layers, though, a does not vary much with thickness. The power-law region occurs when the dipole moments of the surface covering layer have aligned themselves to the N-V center. Thus, the power law of a liquid-covered diamond seems to be more strongly affected by the stability of aligned dipole moments than that of a solid-covered diamond.

Figure 4 shows the noise spectra with thick (1 μm) surface protective layers. The thickness of the protective layer does not change the noise-spectrum transition frequency f_t, since the transition is governed by the relaxation time. However, a thick surface-protective layer does increase the noise floor in general.

The exception to this rule is for those materials with a very short relaxation time τ_{surf}, such as PC and DMSO, and only in the low-frequency range (the noise floor is high for the high-frequency range). This puzzling phenomenon can be explained when we re-express $\bar{S}(\omega)$ in

TABLE II. The noise-power exponent of seven materials examined with thickness 1 nm and 1 μm.

Material	a ($d = 5$ nm)	a ($d = 1$ μm)
PC	−1.6	−0.91
Glycerin	−0.5	−0.15
Silicon	−1.89	−1.92
DMSO	−1.9	−1.1
PFPE	−1.6	−0.2
PMMA	−2.2	−2.1
PVDF	−2.0	−1.94

Eq. (4) by explicitly writing the effective capacitance in terms of geometry and factoring out thickness-independent terms. After some simplification, we obtain

$$\bar{S}(\omega) \approx \Gamma \left(\frac{b_L}{\varepsilon_H'} \frac{d_L}{d_H} \phi_L + \frac{b_H}{\varepsilon_H'} \phi_H \right). \tag{9}$$

where Γ incorporates all factors independent of the layer thickness. The first term of Eq. (9) contains the ratio of the thicknesses of the protective layer and the top diamond layer; it is the only thickness-dependent part of the equation. Note, however, that this first term also depends on the loss tangent. As a result, in materials such as PC and DMSO, the loss tangent ϕ_L of which is much smaller at low frequencies than that of diamond, the first term will be negligible compared to the second term. Thus, in these materials, the thickness makes almost no difference to the noise spectrum at low frequencies, as seen in Fig. 4.

E. Which cover layers reduce noise most effectively?

Having highlighted the roles of four parameters—the relaxation time, loss tangent, power law, and thickness—in noise reduction, we now draw out some practical implications of our results. At low frequencies, fluctuations in

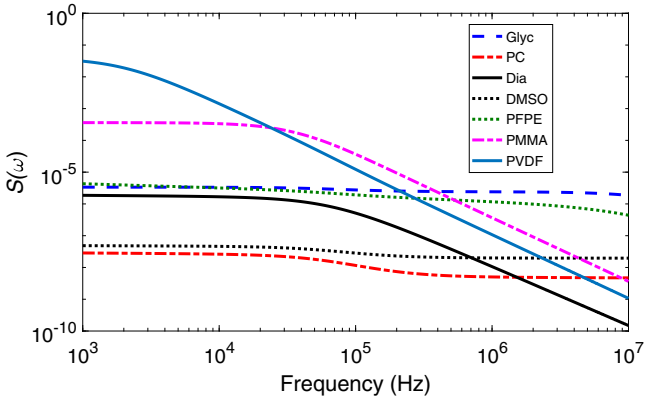

FIG. 4. The noise spectrum with thickness 1 μm. Thicker surface layers have a higher noise floor. The power-law exponent changes with thickness for liquid-surface layers but remains almost the same for solid-surface layers.

dipole-dipole interactions manifest as white noise. Because its characteristic relaxation time is shorter than that of diamond, a thin (<10 nm) protective layer can reduce noise by decreasing the effective loss tangent. In the frequency range under study, liquid surface layers reduce noise more effectively than solid surface layers because the picosecond-to-nanosecond relaxation times of liquids are much shorter than the microsecond relaxation times of solids. Because they can move more easily than in solids, the dipoles in liquids realign more quickly than the dipoles in solids. The low mobility in solids and the consequently slower realignment of dipoles leads to more fluctuation noise. On the other hand, the power-law coefficient in liquids is generally smaller than in solids, and the frequency range over which the power law holds is narrower in liquids than in solids. In liquids, the noise spectrum becomes flat again at frequencies beyond a few megahertz (10^6 Hz), whereas in solids the power law persists even at higher frequencies. As a result, at high frequencies ($>10^7$ Hz), solid protective layers outperform liquid protective layer in noise reduction. Furthermore, the thickness of the surface layer also affects the amount of noise: the thinner the protective layer, the better the noise reduction. A solid protective surface thicker than 10 nm may increase noise rather than reduce it.

IV. CONCLUSIONS

We study the effectiveness in reducing surface noise of protecting layers on N-V-center diamonds. We assume that the main source of the noise is thermally activated surface-charge fluctuations. This assumption is reasonable, since the N-V-center-based devices in question operate at room temperature and various experiments indicate that the noise mainly originates from the electric field [32,48]. We use the quantum fluctuation-dissipation theorem to calculate the noise spectrum. We analyze the noise spectra for six materials commonly used to cover the surface of N-V-center diamonds: glycerol, propylene carbonate, polymethyl methacrylate, polyvinylindene fluoride, perfluoropolyether, and dimethyl sulfoxide. The covering materials examined in this work all exhibit optical transparency in N-V-center experiments and do not interfere with the N-V-center read-out [54–57]. While chemical reactivity with biomolecules for sensing could possibly be affected by the coating, the reduction in noise may more than compensate for this effect.

Our results show that four parameters affect the noise spectra: the effective relaxation time, the effective loss tangent, the exponent of the power law, and the thickness of the surface layer. (The effective capacitance also influences the overall noise spectra, but to a much smaller extent.) Of these four parameters, the effective relaxation time, the effective loss tangent, and the coefficient of the power law determine the shape of the noise spectra, while the thickness of the surface layer determines the overall amount of noise. The effective relaxation time τ_{eff} determines the transition frequency of the noise spectrum: the longer the relaxation time, the lower the transition frequency. The power-law behavior is associated with the stability of aligned dipole moments. Thus solid cover materials have higher power-law exponents (around -2) that are very little influenced by the thickness, while liquid cover materials exhibit a drastic decrease in the power-law coefficient as the thickness increases. Consequently, one can control the power-law behavior by adjusting the cover-layer thickness, if a liquid covering layer is used. The amount of white noise is determined by a combination of the effective loss tangent and the thickness. In addition, the overall charge-fluctuation noise is proportional to the loss tangent and thus the surface noise is worse for so-called "lossy materials." In general, the noise floor increases considerably with increasing thickness. The only exceptions to this rule are materials with very short relaxation times, such as PC and DMSO, and only in low frequency ranges. The thickness of the surface layer does not affect the transition frequency from the white noise to a power law of the noise spectrum.

Our study of six experimentally representative covering materials shows that most covering materials commonly used by experimentalists can reduce noise in the frequency range of 10^3–10^7 Hz. Liquid surface layers reduce noise better overall than solid layers, because their relaxation times are shorter. The ideal material for reducing N-V-center surface noise would be a thin liquid layer with a low real permittivity and a fast (picosecond-range) relaxation time in the frequency range 10^3–10^7 Hz. Solid materials in general are noisier, but their high power-law exponents compensate for the substantial white noise and provide better noise reduction at high frequencies ($>10^7$ Hz).

It should be noted that PMMA is shown to enhance emission that might result in a reduction in lifetime [72]. However, due to the complexity of the nanodiamond tip structure, such measurements may not be directly applicable to our study: in our case, the N-V center is embedded in the bulk diamond.

Finally, the electronic field noise will decrease the T_2 coherence time just as magnetic-field noise does. Since some experiments such as [9,32] show that the electric-field noise and the magnetic-field noise are comparable, reducing the electric-field noise might extend the T_2 time considerably.

ACKNOWLEDGMENTS

We thank Pauli Kehayias and others in Ron Walsworth's group at Harvard for useful discussions and for providing experimental insights. DHS is grateful to ITAMP for hosting her visit during the summer and for providing a

stimulating research environment. This work is supported by NSF Grant No. DMR-1505641.

APPENDIX: DERIVATION OF THE NOISE SPECTRUM

In this appendix, we derive the noise spectrum via the fluctuation-dissipation theorem. We treat the dipole-dipole interaction Hamiltonian between the liquid and the N-V center as the perturbation

$$\delta H = -\mathbf{p}\cdot\mathbf{E}, \tag{A1}$$

where $\mathbf{p}$ is the electric dipole moment between the charges in the covering liquid and the N-V center and $\mathbf{E}$ is the electric field. We treat the interaction using the electric dipole approximation. At thermal equilibrium, the ensemble average of the dipole moment is defined as follows:

$$\langle\mathbf{p}\rangle \equiv \langle\mathbf{p}\,(\mathbf{r},t)\rangle = \frac{\int f_{\mathrm{eq}}\,(\mathbf{r})\,\mathbf{p}\,(\mathbf{r},t)\,dr}{\int f_{\mathrm{eq}}\,(\mathbf{r})\,dr}, \tag{A2}$$

where f_{eq} is the distribution function

$$f\ (x) = f_{\mathrm{eq}} e^{-(\delta H/k_B T)}, \tag{A3}$$

in which k_B is the Boltzmann constant, T is the temperature, the integration runs over all coordinates because the system is at equilibrium, and t is time. The fluctuation is regarded as a system that has been perturbed by $\delta\mathbf{p}$:

$$\delta\mathbf{p} = \mathbf{p} - \langle\mathbf{p}\rangle\,. \tag{A4}$$

This perturbation is small and is linearly dependent on $\mathbf{E}$. This dependence can be given by linear response function theory [73–75],

$$\delta p_j\ (t) = \frac{1}{2\pi}\sum_k \int_{-\infty}^{t} \tilde{\alpha}_{jk}\left(t-t'\right) E_k\left(t'\right) dt'. \tag{A5}$$

Here, $\tilde{\alpha}_{jk}$ is the response function of the system and $j,k = x,y,z$. We have assumed that the system is stationary (i.e., the response function is local) and that the dependence on $t-t'$ enforces causality. The "memory" of the system is contained in $\tilde{\alpha}_{jk}$ and we need to determine $\tilde{\alpha}_{jk}$.

The time dependence of the electric-field perturbation is a step function to ensure complete relaxation of the system at time $t=0$, and the perturbation occurs $[0,\infty)$ with $E = E^0_{\mathbf{k}}$ at $t>0$. Evaluating Eq. (A5) for the step function perturbation, we obtain

$$\delta p_j\ (t) = \frac{E^0_k}{2\pi}\int_t^{\infty} \tilde{\alpha}_{jk}\,(\tau)\,d\tau, \tag{A6}$$

where $\tau \equiv t-t'$. Solving for $\tilde{\alpha}_{jk}$, we obtain

$$\tilde{\alpha}_{jk}\,(t) = -\frac{2\pi}{E^0_k}\Theta(t)\frac{d}{dt}\delta p_j\ (t)\,. \tag{A7}$$

We assume that $\tilde{\alpha}_{jk}\,(t)$ and its time derivative tend to zero as $t\to\infty$ and $\Theta(t)$ is the Heaviside step function to ensure causality. Since the ensemble average is independent of time,

$$\tilde{\alpha}_{jk}\,(t) = -\frac{2\pi}{E^0_k}\Theta(t). \tag{A8}$$

At time $t=0$, the system is in thermal equilibrium. Expanding the exponential in a series, plugging it into Eq. (A2), and keeping only the terms up to linear order in δH, we obtain

$$\mathbf{p} = \langle\mathbf{p}\rangle - \frac{1}{k_B T}\left[\langle\delta H\,(s)\,\mathbf{p}\,(s,t)\rangle - \langle\mathbf{p}\,(s,t)\rangle\,\langle\delta H\,(s)\rangle\right]. \tag{A9}$$

Since $\delta H\,(s)$ is the perturbation at time $t=0$, we have $\delta H\,(s) = -\mathbf{p}\,(s,0)\,E^0_{\mathbf{k}}$ and Eq. (A9) becomes

$$\delta p\ (t) = \frac{E^0_{\mathbf{k}}}{k_B T}\left\langle\delta p_k\,(0)\,\delta p_j\ (t)\right\rangle. \tag{A10}$$

Inserting this result into Eq. (A7), we find

$$\tilde{\alpha}_{jk}\,(t) = \frac{2\pi}{k_B T}\Theta(t)\frac{d}{dt}\left\langle\delta p_k\,(0)\,\delta p_j\ (t)\right\rangle. \tag{A11}$$

It is convenient to do a Fourier transform to express Eq. (A11) in the frequency domain with $\tilde{\alpha}_{jk}\,(t)\to\alpha_{jk}\,(\omega)$ and $\delta p\ (t)\to\delta\tilde{p}_j\ (\omega)$. The correlation function in the frequency domain, $\left\langle\delta\tilde{p}_j\ (\omega)\,\delta\tilde{p}^*_k\left(\omega'\right)\right\rangle$, is

$$\begin{aligned}&\left\langle\delta\tilde{p}_j\ (\omega)\,\delta\tilde{p}^*_k\left(\omega'\right)\right\rangle\\ &= \delta\left(\omega-\omega'\right)\frac{1}{2\pi}\int_{-\infty}^{\infty}\left\langle\delta\tilde{p}_k\,(t)\,\delta\tilde{p}^*_j\,(t+\tau)\right\rangle e^{i\omega t}dt.\end{aligned} \tag{A12}$$

To obtain a spectral representation of the fluctuation-dissipation theorem, we need to Fourier transform Eq. (A11). The right-hand side leads to a convolution between the spectrum of the step function $\Theta(t)$ and the spectrum of $d/dt\left\langle\delta p_k\,(0)\,\delta p_j\ (t)\right\rangle$. To remove of the imaginary part of the step function, we solve for $[\alpha_{jk}(\omega)-\alpha^*_{kj}(\omega)]$ instead of $\alpha_{jk}\,(\omega)$. Using the Wiener-Khintchine theorem [76] and taking the real part (note that

$\langle \delta p_k(t)\, \delta p_j(t+\tau) \rangle$ is real), we obtain

$$\left\langle \delta\tilde{p}_j(\omega)\, \delta\tilde{p}_k^*(\omega') \right\rangle = \frac{k_B T}{2\pi i\omega} \left[\alpha_{jk}(\omega) - \alpha_{kj}^*(\omega) \right] \delta(\omega - \omega'). \tag{A13}$$

The Wiener-Khintchine theorem applies to classical systems, where $\hbar\omega \ll k_B T$. However, we can generalize it to quantum systems by replacing $k_B T$ by $\hbar\omega/\left(1 - e^{-\hbar\omega/k_B T}\right)$ and substituting into Eq. (A13). Then $\left\langle \delta\tilde{p}_j(\omega)\, \delta\tilde{p}_k^*(\omega') \right\rangle$ becomes

$$\left\langle \delta\tilde{p}_j(\omega)\, \delta\tilde{p}_k^*(\omega') \right\rangle = \frac{1}{2\pi i\omega} \left[\frac{\hbar\omega}{1 - e^{-\hbar\omega/k_B T}} \right] \times \left[\alpha_{jk}(\omega) - \alpha_{kj}^*(\omega) \right] \delta(\omega - \omega'). \tag{A14}$$

Fluctuation is now converted to dissipation on the right-hand side. We now need to determine $\alpha_{jk}(\omega) - \alpha_{kj}^*(\omega)$. Dissipation in the system is associated with the imaginary part of the complex electric susceptibility, χ_e'', since $p \propto \varepsilon_0 \chi_e$, where ε_0 is the vacuum permittivity and χ_e is the complex electric susceptibility. Therefore, the dissipation term is contained in χ_e'', and $\alpha_{jk}(\omega)$ is thus $i\varepsilon_0 \chi_e''$.

The noise spectrum is obtained from the fluctuation of the dipole moment by plugging $\alpha_{jk}(\omega) = i\varepsilon_0 \chi_e''$ into Eq. (A14) and then into Eq. (2):

$$S(\mathbf{k}, \omega) = 2 \int_{-\infty}^{\infty} \left\langle \delta p(\mathbf{r}, \tau) \delta p(\mathbf{r}', \tau + t) \right\rangle e^{-i\omega t} dt. \tag{A15}$$

However, since the system's response function is local, fluctuations at distinct spatial coordinates are uncorrelated. Then $\delta p(\mathbf{r}, \tau) = \delta p(\tau)$ and $S(\mathbf{k}, \omega) = S(\omega)$, so that

$$S(\omega) = \frac{4\hbar}{1 - e^{-\hbar\omega/k_B T}} \varepsilon_0 \chi_e''. \tag{A16}$$

[1] L. Childress, R. Walsworth, and M. Lukin, Atom-like crystal defects: From quantum computers to biological sensors, Phys. Today **67**, 38 (2014).

[2] Z. Xiang, S. Ashhab, J. Q. You, and F. Nori, Hybrid quantum circuits: Superconducting circuits interacting with other quantum systems, Rev. Mod. Phys. **86**, 623 (2013).

[3] G. Balasubramanian, P. Neumann, D. Twitchen, M. Markham, R. Kolesov, N. Mitzuochi, J. Isoya, J. Achard, J. Beck, J. Tissler, V. Jacques, P. R. Hemmer, F. Jelezko, and J. Wrachtrup, Ultralong spin coherence time in isotopically engineered diamond, Nat. Mater. **8**, 383 (2009).

[4] G. Balasubramanian, I. Y. Chan, R. Kolesov, M. Al-Hmoud, J. Tissler, C. Shin, C. Kim, A. Wojcik, P. R. Hemmer, A. Krueger, T. Hanke, A. Leitenstorfer, R. Bratschitsch, F. Jelezko, and J. Wrachtrup, Nanoscale imaging magnetometry with diamond spins under ambient conditions, Nature **455**, 648 (2008).

[5] J. R. Maze, P. L. Stanwix, J. S. Hodges, S. Hong, J. M. Taylor, P. Cappellaro, L. Jiang, M. V. Gurudev Dutt, E. Togan, A. S. Zibrov, A. Yacoby, R. L. Walsworth, and M. D. Lukin, Nanoscale magnetic sensing with an individual electronic spin in diamond, Nature **455**, 644 (2008).

[6] M. S. Grinolds, S. Hong, P. Malentinsky, L. Luan, M. D. Lukin, R. L. Walsworth, and A. Yacoby, Nanoscale magnetic imaging of a single electron spin under ambient conditions, Nat. Phys. **9**, 215 (2013).

[7] E. Togan, Y. Chu, A. S. Trifonov, L. Liang, J. Maze, L. Childress, M. V. G. Dutt, A. S. Sorensen, P. R. Hemmer, A. S. Zibrov, and M. D. Lukin, Quantum entanglement between an optical photon and a solid-state spin qubit, Nature **466**, 730 (2010).

[8] G. Waldherr, P. Neumann, S. F. Huelga, F. Jelezko, and J. Wrachtrup, Violation of a Temporal Bell Inequality for Single Spins in a Diamond Defect Center, Phys. Rev. Lett. **107**, 090401 (2011).

[9] B. A. Myers, A. Ariyaratne, and A. C. Bleszynski Jayich, Double-Quantum Spin-Relaxation Limits to Coherence of Near-Surface Nitrogen-Vacancy Centers, Phys. Rev. Lett. **118**, 197201 (2017).

[10] K. D. Jahnke, B. Naydenov, T. Teraji, S. Koizumi, T. Umeda, J. Isoya, and F. Jelezko, Long coherence time of spin qubits in ^{12}C enriched polycrystalline chemical vapor deposition diamond, Appl. Phys. Lett. **101**, 012405 (2012).

[11] M. W. Doherty, V. M. Acosta, A. Jarmola, M. S. J. Barson, N. B. Manson, D. Budker, and L. C. L. Hollenberg, Temperature shifts of the resonances of the NV center in diamond, Phys. Rev. B **90**, 041201(R) (2014).

[12] A. Laraoui, F. Dolde, C. Burk, F. Reinhard, J. Wrachtrup, and C. A. Meriles, High-resolution correlation spectroscopy of ^{13}C spins near a nitrogen-vacancy centre in diamond, Nat. Commun. **4**, 1651 (2013).

[13] J. M. Taylor, P. Cappelaro, L. Childress, L. Jiang, D. Budker, P. R. Hemmer, A. Yacoby, R. Walsworth, and M. D. Lukin, High-sensitivity diamond magnetometer with nanoscale resolution, Nat. Phys. **4**, 810 (2008).

[14] C. L. Degan, Scanning magnetic field microscope with a diamond single-spin sensor, Appl. Phys. Lett. **92**, 243111 (2008).

[15] V. M. Acosta, E. Bauch, M. P. Ledbetter, C. Santori, K. M. C. Fu, P. E. Barclay, R. G. Beausoleil, H. Linget, J. F. Roch, F. Treussart, S. Chemerisov, W. Gawlik, and D. Budker, Diamonds with a high density of nitrogen-vacancy centers for magnetometry applications, Phys. Rev. B **80**, 115202 (2009).

[16] A. Jarmola, Z. Bodrog, P. Kehayias, M. Markham, J. Hall, D. J. Twitchen, V. M. Acosta, A. Gali, and D. Budker, Optically detected magnetic resonances of nitrogen-vacancy ensembles in ^{13}C-enriched diamond, Phys. Rev. B. **94**, 094108 (2016).

[17] F. Dolde, H. Fedder, M. W. Doherty, T. Nöbauer, F. Rempp, G. Balasubramanian, T. Wolf, F. Reinhard, L. C. Hollenberg, F. Jelezko, and J. Wrachtrup, Electric-field sensing using single diamond spins, Nat. Phys. **7**, 459 (2011).

[18] M. W. Doherty, F. Dolde, H. Fedder, F. Jelezko, J. Wrachtrup, N. B. Manson, and L. C. L. Hollenberg,

Theory of the ground-state spin of the NV^- center in diamond, Phys. Rev. B **85**, 205203 (2012).

[19] F. Dolde, M. W. Doherty, J. Michl, I. Jakobi, B. Naydenov, S. Pezzagna, J. Meijer, P. Neumann, F. Jelezko, N. B. Manson, and J. Wrachtrup, Nanoscale Detection of a Single Fundamental Charge in Ambient Conditions using the NV^- Center in Diamond, Phys. Rev. Lett. **112**, 097603 (2014).

[20] P. Ovartchaiyapong, K. W. Lee, B. A. Myers, and A. C. B. Jayich, Dynamic strain-mediated coupling of a single diamond spin to a mechanical resonator, Nat. Commun. **5**, 4429 (2014).

[21] E. R. MacQuarrie, T. A. Gosavi, N. R. Jungwirth, S. A. Bhave, and G. D. Fuchs, Mechanical Spin Control of Nitrogen-Vacancy Centers in Diamond, Phys. Rev. Lett. **111**, 227602 (2013).

[22] D. M. Toyli, C. F. de las Casas, D. J. Christle, V. V. Dobrovitski, and D. D. Awschalom, Fluorescence thermometry enhanced by the quantum coherence of single spins in diamond, Proc. Natl. Acad. Sci. U.S.A. **110**, 8417 (2013).

[23] G. Kucsko, P. C. Maurer, N. Y. Yao, M. Kubo, H. J. Noh, P. K. Lo, H. Park, and M. D. Lukin, Nanometre-scale thermometry in a living cell, Nature **500**, 54 (2013).

[24] P. Neumann, N. Mizouchi, F. Rempp, P. Hemmer, H. Watanabe, S. Yamasaki, V. Jacques, T. Gaebel, F. Jelezko, and J. Wrachtrup, Multipartite entanglement among single spins in diamond, Science **320**, 1326 (2008).

[25] P. Neumann, R. Kolesov, B. Naydenov, J. Beck, F. Rempp, M. Steiner, V. Jacques, G. Balasubramanian, M. L. Markham, D. J. Twitchen, S. Pezzagna, J. Meijer, J. Twamley, F. Jelezko, and J. Wrachtrup, Quantum register based on coupled electron spins in a room-temperature solid, Nat. Phys. **6**, 249 (2010).

[26] P. Neumann, J. Beck, M. Steiner, F. Rempp, H. Fedder, P. R. Hemmer, J. Wrachtrup, and F. Jelezko, Single-shot readout of a single nuclear spin, Science **329**, 542 (2010).

[27] G. Waldherr, J. Beck, M. Steiner, P. Neumann, A. Gali, Th. Frauenheim, F. Jelezko, and J. Wrachtrup, Dark States of Single Nitrogen-Vacancy Centers in Diamond Unraveled by Single Shot NMR, Phys. Rev. Lett. **106**, 157601 (2011).

[28] T. Staudacher, F. Shi, S. Pezzagna, J. Meijer, J. Du, C. A. Meriles, F. Reinhard, and J. Wrachtrup, Nuclear magnetic resonance spectroscopy on a (5-nanometer)^3 sample volume, Science **339**, 561 (2013).

[29] D. Rugar, H. J. Mamin, M. H. Sherwood, M. Kim, C. T. Rettner, K. Ohno, and D. D. Awschalom, Proton magnetic resonance imaging using a nitrogen-vacancy spin sensor, Nat. Nanotechnol. **10**, 120 (2015).

[30] T. H"aberle, D. Schmid-Lorch, F. Reinhard, and J. Wrachtrup, Nanoscale nuclear magnetic imaging with chemical contrast, Nat. Nanotechnol. **10**, 125 (2015).

[31] M. Kim, H. J. Mamin, M. H. Sherwood, C. T. Rettner, J. Frommer, and D. Ruger, Ultrafast magnetization switching by spin-orbit torques, Appl. Phys. Lett. **105**, 042406 (2014).

[32] M. Kim, H. J. Mamin, M. H. Sherwood, K. Ohno, D. D. Awschalom, and D. Rugar, Decoherence of Near-Surface Nitrogen-Vacancy Centers Due to Electric Field Noise, Phys. Rev. Lett. **115**, 087602 (2015).

[33] F. Fávaro de Oliveira, S. Momenzadeh, D. Antonov, H. Fedder, A. Denisenk, and J. Wrachtrup, On the efficiency of combined ion implantation for the creation of near-surface nitrogen-vacancy centers in diamond, Phys. Status Solidi A **8**, 2044 (2016).

[34] T. Rosskopf, A. Dussaux, K. Ohashi, M. Loretz, R. Schirhagl, H. Watanabe, S. Shikata, K. M. Itoh, and C. L. Degen, Investigation of Surface Magnetic Noise by Shallow Spins in Diamond, Phys. Rev. Lett. **112**, 147602 (2014).

[35] B. A. Myers, A. Das, M. C. Dartiailh, K. Ohno, D. D. Awschalom, and A. C. Bleszynski Jayich, Probing Surface Noise with Depth-Calibrated Spins in Diamond, Phys. Rev. Lett. **113**, 027602 (2014).

[36] B. K. Ofori-Okai, S. Pezzagna, K. Chang, M. Loretz, R. Schirhagl, Y. Tao, B. A. Moores, K. Groot-Berning, J. Meijer, and C. L. Degen, Spin properties of very shallow nitrogen vacancy defects in diamond, Phys. Rev. B **86**, 081406(R) (2012).

[37] R. De Sousa, Dangling-bond spin relaxation and magnetic $1/f$ noise from the amorphous-semiconductor/oxide interface: Theory, Phys. Rev. B **76**, 245306 (2007).

[38] N. Bar-Gill, L. Pham, C. Belthangady, D. Le Sage, P. Cappellaro, J. Maze, M. Lukin, A. Yacoby, and R. Walsworth, Suppression of spin-bath dynamics for improved coherence of multi-spin-qubit systems, Nat. Commun. **3**, 858 (2012).

[39] N. Bar-Gill, L. M. Pham, A. Jarmola, D. Budker, and R. L. Walsworth, Solid-state electronic spin coherence time approaching one second, Nat. Commun. **4**, 1743 (2013).

[40] V. Y. Osipov, A. Shames, and A. Y. Vul', Exchange coupled pairs of dangling bond spins as a new type of paramagnetic defects in nanodiamonds, Phys. B: Condens. Matter **404**, 4522 (2009).

[41] N. D. Samsonenko, G. V. Zhmykhov, V. S. Zon, and V. K. Aksenov, Characteristic features of the electron paramagnetic resonance of the surface centers of diamond, J. Struct. Chem. **20**, 951 (1980).

[42] J. Tisler, G. Balasubramanian, B. Naydenov, R. Kolesov, B. Grotz, R. Reuter, J.-P. Boudou, P. A. Curmi, M. Sennour, A. Thorel *et al.*, Fluorescence and spin properties of defects in single digit nanodiamonds, ACS Nano **3**, 1959 (2009).

[43] L. P. McGuinness, L. T. Hall, A. Stacey, D. A. Simpson, C. D. Hill, J. H. Cole, K. Ganesan, B. C. Gibson, S. Prawer, P. Mulvaney *et al.*, Ambient nanoscale sensing with single spins using quantum decoherence, New J. Phys. **15**, 073042 (2013).

[44] R. C. Bansal, F. J. Vastola, and P. L. Walker, Kinetics of chemisorption of oxygen on diamond, Carbon **10**, 443 (1972).

[45] H. Bluhm, J. A. Bert, N. C. Koshnick, M. E. Huber, and K. A. Moler, Spinlike Susceptibility of Metallic and Insulating Thin Films at Low Temperature, Phys. Rev. Lett. **103**, 026805 (2009).

[46] K. Ohashi, T. Rosskopf, H. Watanabe, M. Loretz, Y. Tao, R. Hauert, S. Tomizawa, T. Ishikawa, J. Ishi-Hayase, S. Shikata, C. L. Degen, and K. M. Itoh, Negatively charged nitrogen-vacancy centers in a 5 nm thin ^{12}C diamond film, Nano Lett. **13**, 4733 (2013).

[47] K. Ohno, F. Joseph Heremans, L. C. Bassett, B. A. Myers, D. M. Toyli, A. C. Bleszynski Jayich, C. J. Palmstrom, and D. D. Awschalom, Engineering shallow spins in diamond with nitrogen delta-doping, Appl. Phys. Lett. **101**, 082413 (2012).

[48] Y. Romach, C. Müller, T. Unden, L. J. Rogers, T. Isoda, K. M. Itoh, M. Markham, A. Stacey, J. Meijer, S. Pezzagna, B. Naydenov, L. P. McGuinness, N. Bar-Gill, and F. Jelezko, Spectroscopy of Surface-Induced Noise Using Shallow Spins in Diamond, Phys. Rev. Lett. **114**, 017601 (2015).

[49] H. J. Mamin, M. Kim, M. H. Sherwood, C. T. Rettner, K. Ohno, D. D. Awschalom, and D. Rugar, Nanoscale nuclear magnetic resonance with a nitrogen-vacancy spin sensor, Science **339**, 557 (2013).

[50] P. Kehayais, A. Jarmola, N. Mosavain, I. Fescenko, F. M. Benito, A. Laraoui, J. Smits, L. Bougas, D. Budker, A. Neumann, S. R. J. Brueck, and V. M. Acosta, Solution nuclear magnetic resonance spectroscopy on a nanostructured diamond chip, Nat. Commun. **8**, 188 (2017).

[51] D. R. Glenn, D. B. Bucher, J. Lee, M. D. Lukin, H. Park, and R. L. Walsworth, High resolution magnetic resonance spectroscopy using solid-state spin sensor, Nature **555**, 351 (2018).

[52] N. Aslam, M. Pfender, P. Neumann, R. Reuter, A. Zappe, F. F. Oliveira, A. Denisko, H. Sumiya, S. Onoda, J. Isoya, and J. Wrachtrup, Nanoscale nuclear magnetic resonance with chemical resolution, Science **7**, 6346 (2017).

[53] S. Kuehn, R. F. Loring, and J. A. Marohn, Dielectric Fluctuations and the Origins of Noncontact Friction, Phys. Rev. Lett. **96**, 156103 (2006).

[54] H. M. Zidan, and M. Abu-Elnader, Structural and optical properties of pure PMMA and metal chloride-doped PMMA films, Phys. B: Condens. Matter **355**, 308 (2005).

[55] C. Duan, W. N. Mei, W. Yin, J. Liu, J. R. Hardy, M. Bai, and S. Ducharme, Theoretical study on the optical properties of polyvinylidene fluoride crystal, J. Phys. Condens. Matter **15**, 3805 (2003).

[56] W. Jones, Jr., Properties of perfluoropolyethers for space applications, NASA-TM-106616, 19940033009 (1994).

[57] K. A. Akmarov, S. N. Lapshov, and A. S. Sherstobitova, Optical properties of aqueous solutions of dimethyl sulfoxide and application of refractometry for monitoring their composition, J. Appl. Spectrosc. **80**, 610 (2013).

[58] S. Havriliak, and S. Negami, A complex plane representation of dielectric and mechanical relaxation processes in some polymers, Polymer **8**, 161 (1967).

[59] M. Principe, I. M. Pinto, V. Pierro, R. DeSalvo, I. Taurasi, A. E. Villar, E. D. Black, K. G. Libbrecht, C. Michel, N. Morgado, and L. Pinard, Material loss angles from direct measurements of broadband thermal noise, Phys. Rev. D **91**, 022005 (2015).

[60] A. E. Villar, E. D. Black, R. DeSalvo, K. G. Libbrecht, C. Michel, N. Morgado, L. Pinard, I. M. Pinto, V. Pierro, V. Galdi, M. Principe, and I. Taurasi, Measurement of thermal noise in multilayer coatings with optimized layer thickness, Phys. Rev. D **81**, 122001 (2010).

[61] G. Harry, A. Gretarsson, P. Saulson, S. Kittelberger, S. Penn, W. Startin, S. Rowan, M. Fejer, D. R. M. Crooks, G. Cagnoli, J. Hough, and N. Nakagawa, Thermal noise in interferometric gravitational wave detectors due to dielectric optical coatings, Class. Quantum Grav. **19**, 897 (2002).

[62] G. Harry, H. Armandula, E. Black, D. R. M. Crooks, G. Cagnoli, J. Hough, P. Murray, S. Reid, S. Rowan, P. Sneddon, M. Fejer, R. Route, and S. Penn, Thermal noise from optical coatings in gravitational wave detectors, Appl. Optics **45**, 1569 (2006).

[63] A. N. Brozdnichenko, D. M. Dolgintsev, and R. A. Castro, The dielectric properties of the diamond-like films grown by ion-plasma method, J. Phys.: Conf. Ser. **572**, 012025 (2014).

[64] M. Köhler, P. Lunkenheimer, and A. Loidl, Dielectric and conductivity relaxation in mixtures of glycerol with LiCl, Eur. Phys. J. E **27**, 115 (2008).

[65] X. You, M. I. Chaudhari, S. B. Rempe, and L. R. Pratt, Dielectric relaxation of ethylene carbonate and propylene carbonate from molecular dynamics simulations, J. Phys. Chem. B **120**, 1849 (2016).

[66] M. G. Giri, M. Carla, C. M. C. Gambi, D. Senatra, A. Chittofrati, and A. Sanguineti, Dielectric permittivity measurements on highly conductive perfluoropolyether microemulsions at frequencies up to 100 MHz, Meas. Sci. Technol. **4**, 627 (1993).

[67] V. M. Boucher, D. Cangialosi, A. Alegria, J. Colmenero, J. Gonzalez-Irun, and L. M. Liz-Marzan, Physical aging in PMMA/silica nanocomposites: Enthalpy and dielectric relaxation, J. Non-Cryst. Solids **347**, 605 (2011).

[68] P. Thomas, K. T. Varughese, K. Dwarakanath, and K. B. R. Varma, Dielectric properties of Poly(vinylidene fluoride)/$CaCu_3Ti_4O_{12}$ composites, Comp. Sci. and Tech. **70**, 539 (2010).

[69] K. Schröter, S. A. Hutcheson, X. Shi, A. Mandanici, and G. B. Mckenna, Dynamic shear modulus of glycerol: Corrections due to instrument compliance, J. Chem. Phys. **125**, 214507 (2006).

[70] A. P. Gregory and R. N. Clarke, Tables of the complex permittivity of dielectric reference liquids at frequencies up to 5 GHz, NPL Report MAT **23** (2012).

[71] A. Safavi-Naini, P. Rabl, P. F. Weck, and H. R. Sadeghpour, Microscopic model of electric-field-noise heating in ion traps, Phys. Rev. A **84**, 023412 (2011).

[72] A. Khalid, K. Chung, R. Rajasekharan, D. W. M. Lau, T. J. Karle, B. C. Gibson, and S. Tomljenovic-Hanic, Lifetime reduction and enhanced emission of single photon color centers in nanodiamond via surrounding refractive index modification, Sci. Rep. **5**, 11179 (2015).

[73] G. S. Agarwal, Quantum electrodynamics in the presence of dielectrics and conductors. I. Electromagnetic-field response functions and black-body fluctuations in finite geometries, Phys. Rev. A **11**, 230 (1975).

[74] C. Henkel, K. Joulain, J.-P. Mulet, and J.-J. Greffet, Radiation forces on small particles in thermal near fields, J. Opt. A: Pure Appl. Opt. **4**, S109 (2002).

[75] J. M. Wylie, and J. E. Sipe, Quantum electrodynamics near an interface, Phys. Rev. A **30**, 1185 (1984).

[76] M. Constantin, C. C. Yu, and J. M. Martinis, Saturation of two-level systems and charge noise in Josephson junction qubits, Phys. Rev. B **79**, 094520 (2009).